Overexpression of kinesin superfamily motor proteins in Alzheimer's disease

Running title: Overexpression of KIFs in AD

Dr Kelly Hares[a] (BSc, PhD), Dr James Scott Miners[b] (BSc, PhD), Miss Amelia Jane Cook[a], Dr Claire Rice[a] (FRCP, PhD), Professor Neil Scolding[a] (FRCP, PhD), Professor Seth Love[b] (FRCPath, PhD) and Dr Alastair Wilkins[a] (FRCP, PhD).

[a]School of Clinical Sciences, MS and Stem Cell Group, University of Bristol, BS10 5NB, UK.

[b]School of Clinical Sciences, Dementia Research Group, University of Bristol, BS10 5NB, UK.

Correspondence:

Dr Kelly Hares, MS and Stem Cell Group, 1st Floor, Clinical Neurosciences Office, Learning and Research Building, Southmead Hospital, Bristol, BS10 5NB, UK.

E-mail: kelly.hares@bristol.ac.uk

Tel: 0117 414 7804

Fax: 0117 4147838

Abstract

Defects in motor protein-mediated neuronal transport mechanisms have been implicated in a number of neurodegenerative disorders but remain relatively little studied in Alzheimer's disease (AD). Our aim in the present study was to assess the expression of the anterograde kinesin superfamily motor proteins KIF5A, KIF1B and KIF21B, and to examine their relationship to levels of hyperphosphorylated tau, amyloid-β protein precursor (AβPP) and amyloid-β (Aβ) in human brain tissue. We used a combination of qPCR, immunoblotting and ELISA to perform these analyses in midfrontal cortex from 49 AD and 46 control brains. Expression of KIF5A, KIF1B and KIF21B at gene and protein level was significantly increased in AD. KIF5A protein expression correlated inversely with the levels of AβPP and soluble Aβ in AD brains. Upregulation of KIFs may be an adaptive response to impaired axonal transport in AD.

Keywords: Alzheimer's disease, kinesin, amyloid, tau

Introduction

Neuronal health in the central nervous system is dependent on a range of physiological processes which maintain cellular structure, ion homeostasis, electrical activity and synaptic function. The transport of cellular organelles and proteins throughout the neuron, including along the axon and dendrites, is crucial for maintenance of neuronal structure and function. Defects in motor protein-mediated neuronal transport mechanisms have been implicated in a number of neurodegenerative disorders [1].

Transport within neurons is mediated by multiple motor proteins, many of which are involved in synaptic transmission and axonal trafficking. Kinesin superfamily proteins (KIFs) comprise a large group of motor proteins whose primary role is the anterograde axonal transport and intraneuronal transport of protein cargoes through association with microtubule 'rails' [2]. Currently, there are 45 known members of the KIF family, 38 of which are neuronally enriched [3]. The majority of KIFs have an NH_2-terminal head, comprising a microtubule binding domain and a conserved globular motor domain which hydrolyses ATP to produce the energy required for movement of cargoes along the microtubule and through the axon. The head is attached by an α-helical stalk to a COOH-terminal (tail) to which cargoes bind [2, 4]. In most cases, the tail domain of each KIF determines its cargo specificity. In terms of conventional kinesin, cargoes can bind directly or indirectly, through kinesin light chain (KLC) associations and protein adaptor complexes, to the tail domain [5]. Essential neuronal cargoes transported by KIFs include cellular organelles such as mitochondria, pre- and post- synaptic membrane proteins, and a range of structural proteins such as neurofilaments (NFs) [1].

Given the essential role of KIFs in protein trafficking, it is not surprising that mutations in KIFs are associated with neurodegenerative diseases. Point mutations in the KIF5A gene have been linked to several axonopathies including hereditary spastic paraplegia type 10 (SPG-10) [6] and Charcot-Marie Tooth disease type 2A (CMT-2A) [7]. SPG10 is implicated in disturbed intracellular axonal transport and is characterized by axonal loss in the corticospinal tract [6, 8]. Animal gene knock-out studies have also highlighted the importance of KIF5A in axonal transport and neuronal development [9]. In addition, single nucleotide polymorphisms (SNPs) within the KIF5A gene locus (*rs12368653* and *rs703842*) have also been linked to multiple sclerosis (MS) susceptibility [10, 11], and we previously found levels of KIF5A protein in MS tissue to be related to SNP copy number [12, 13]. KIF5A is believed to transport amyloid β precursor protein (AβPP), mitochondria and a range of pre-synaptic membrane proteins that form the SNARE complex [9, 14-18]. The majority of these cargoes bind indirectly to KIF5A through KLCs.

SNPs in the region of the KLC1 gene have been associated with Alzheimer's disease (AD) susceptibility [19]. Andersson *et al* [20] reported that SNPs in KLC1 were associated with APOE ε4 carrier status and with the cerebrospinal fluid level of hyperphosphorylated tau in mild cognitive impairment patients who converted to AD during follow-up; suggesting that variability in axonal transport could influence early AD pathogenesis. In support of this theory, studies using familial AD (FAD) AβPP over-expressing transgenic mice have shown abnormal axonal morphology and large axonal swellings co-positive for KLC and phosphorylated NF-H within 4 months of birth [21]. In addition, transgenic mice with modified presenilin-1 expression have demonstrated reduced affinity between KLC and membrane bound organelles (such as synaptophysin and syntaxin-I containing vesicles), mediated via KLC phosphorylation by elevated glycogen synthase kinase 3β (GSK-3β) activity. Elevated GSK-3β activity has also been directly associated with levels of hyperphosphorylated tau in FAD models [22, 23]. The formation of intraneuronal neurofibrillary tangles (NFTs), composed of aggregated hyperphosphorylated tau protein, is a cardinal feature of AD. Under physiological conditions tau interacts with tubulin as a microtubule stabiliser [24], forming an important contributor to the structure and integrity of the axon for signal conductance. We have previously found reduced KIF5A, KIF1B and KIF21B expression in multiple sclerosis tissue [12] and demonstrated significant inverse correlations between KIF5A and cargo expression, suggesting that lower levels of KIF5A contribute to the axonal aggregation of proteins that lead to the formation of axonal spheroids, commonly seen in the disease [13]. KIF1B and KIF21B were studied as they have been linked to MS susceptibility [25, 26]. KIF1B is believed to share functional redundancy with KIF5A for neuronal protein cargoes and a mutation in its motor domain is also linked to CMT-2A [27]. KIF21B is dendritically enriched and involved in post-synaptic protein transport [28].

As intraneuronal aggregation of proteins is also a feature of AD, a disease in which neuronal protein transport is likely impaired [29], we thought it would be of interest to assess KIF5A, KIF1B and KIF21B expression in AD and to analyse the relationship between these KIF motors and the levels of AβPP, Aβ and hyperphosphorylated tau.

Materials and methods

Study Cohort

Samples of midfrontal cortex (BA 9) cDNA and protein homogenate were obtained from the South West Dementia Brain Bank (Bristol, UK), under the terms of South West - Central Bristol Research Ethics Committee approval no 08/H0106/28+5. We studied 49 cases of AD (in which, according to the National Institute on Aging – Alzheimer's Association criteria [30], AD neuropathological change was an adequate explanation of dementia) and 46 age-matched controls without a history of cognitive impairment (Table 1).

Quantitative real-time PCR (qPCR)

Quantitative real-time qPCR was performed on a StepOnePlus™ Real-Time PCR system with StepOne software v2.1 (Applied Biosystems; Fisher Scientific UK Ltd, Loughborough, UK). Control and AD cDNA samples were used at a concentration of 2 ng/µL, diluted to a final volume of 20 µL with TaqMan® 2x Fast Advanced Master Mix and TaqMan® gene expression assays for KIF5A (Hs01007893_m1), KIF1B (Hs01114538_m1) and KIF21B (Hs01118428_m1; FAM-MGB dye-labelled) (Applied Biosystems). qPCR was performed on a FAST ramp speed holding at 50°C for 2 min, 95°C for 20 s, followed by 40 cycles at 95°C for 1 s and 60°C for 20 s. Gene expression ($2^{-\Delta\Delta ct}$) was calculated relative to the gene encoding the neuron-specific protein NeuN (RBFOX3; Hs01370653_m1; FAM-MGB dye-labelled) and neuron-specific enolase 2 (ENO-2; Hs00157360_m1; FAM-MGB dye-labelled) (Applied Biosystems).

Western blotting

All primary antibodies that we used in dot blots were initially tested for antibody specificity by western blot. Protein homogenates were diluted 1:1 with Laemmli 2x sample buffer (Sigma-Aldrich Ltd; Dorset, UK) and heated to 95°C for 5 min to denature the protein before applying to gels. A Mini-PROTEAN Tetra Cell was constructed with mini-Protean TGX gels (4-20%) (Biorad Hertfordshire, UK). The Tetra Cell chambers were filled with Tris/Glycine/SDS running buffer (Biorad), before we loaded 7 µL BLUeye Prestained Protein Ladder (Geneflow; Staffordshire, UK) and 15 µL of denatured AD protein homogenate in the remaining lanes. The gel was run for approximately 1 h (until the dye front reached the gel bottom) at 150 V. Proteins on the gel were then

transferred onto nitrocellulose membrane for 90 min at 350 mA. Nitrocellulose membrane from the gel transfer was blocked in 5% BSA/Tris-buffered saline-Tween 20 (TBS-T) or 5% milk/TBS-T (depending on antibody), for 1 h at room temperature before its incubation with primary antibody (reconstituted in membrane blocking solution), overnight at 4°C. Primary antibodies used for blotting were as follows: rabbit anti-KIF5A (Sigma-Aldrich Ltd; HPA004469), mouse anti-GAPDH (Abcam; Ab9484); mouse anti-AβPP (Zymed; Life Technologies Ltd; Paisley, UK; 13-0200), rabbit anti-KIF21B (Sigma-Aldrich Ltd; HPA027274), rabbit anti-NEUN (Abcam; Ab177487), mouse anti-PHF-TAU (Invitrogen; Fisher Scientifc UK Ltd; MN1020) and rabbit anti-KIF1B (Bethyl Laboratories; Montgomery, USA; A301-055A). Optimal antibody concentration and the specific blocking solution used are detailed in Table 2. Bound primary antibody was detected by incubation with HRP-conjugated goat anti-rabbit IgG pre-adsorbed (1:10,000; Ab6721) or goat anti-mouse IgG (1:5000; Ab6789) secondary antibodies (both Abcam), for 1 h at room temperature. Protein expression was visualised using a chemiluminescence EZ-ECL kit (1:1; Geneflow), in conjunction with a Biorad Universal III Bioplex imager. Densitometric band analysis was performed using Image Lab™ 5.0 software (Biorad). All antibodies displayed specific bands as described on manufacturer data sheets and consistent with their reported molecular weights (Supplementary Figure 1).

Dot blotting

Dot blotting was performed with antibodies we had validated for specificity by western blot, as listed in Table 2. Nitrocellulose membrane was pre-soaked in 1x TBS, before placement in the 96-well Bio-Dot Microfiltration manifold (Biorad). The manifold was assembled according to the manufacturer's protocol. Frontal lobe protein homogenates were diluted (1:75) with 1x TBS, and 100 µL of each sample (49 AD and 46 control) was transferred by microfiltration for 90 min, including a blank TBS control well. In order to maximise the sample size available on the 96-well manifold, technical replicates were not used. The nitrocellulose membrane was subsequently removed from the manifold for blocking, antibody incubation and chemiluminescence visualisation, as per the western blotting protocol. Densitometric analysis of protein dots was performed using Image Lab™ 5.0 software (Biorad). Integrated density values were expressed relative to the neuronal control protein NeuN.

Tissue preparation for soluble and insoluble (guanidine-extractable) Aβ measurements

Approximately 200 mg of frontal tissue was homogenised in TBS extraction buffer as previously described [31]. In brief, homogenates were centrifuged at 20, 817g for 15 min at 4°C and the supernatant (soluble fraction) stored at −80°C until use. The remaining pellet was homogenised in 6.25 M guanidine HCl (50 mM Tris/HCl (pH 8.0)) and incubated for 4 h at 25°C, followed by centrifugation at 20, 817g for 20 min, at 4°C. The supernatant (guanidine-extractable fraction) was stored at −80°C until use.

Enzyme-linked immunosorbent assay (ELISA)

Sandwich ELISA was used to measure total Aβ in the soluble and insoluble (guanidine-HCl-extractable) fractions of the homogenates, as previously described [32]. Monoclonal anti-Aβ (4G8 clone, raised against amino acids 18-22; Millipore; Watford, UK), was used for the capture step and biotinylated anti-human Aβ monoclonal antibody (10H3 clone) (Thermo Fisher Scientific; Northumberland, UK), for the detection step.

Statistical analysis

Univariate mRNA and protein analysis was carried out using GraphPad Prism5™ (GraphPad Software Inc.; San Diego, USA). Data normality was tested using the Shapiro-Wilk test. Unpaired t-tests or non-parametric Mann-Whitney tests, as appropriate, were used to compare mRNA and protein data between the AD and control cohorts. Parametric Pearson's or non-parametric Spearman's correlation was used to interpret any relationship between proteins. One-way ANOVA with post-hoc Bonferroni was used to analyse KIF data categorised by Braak score. A multiple regression model (STATA v12; StataCorp LLC; Texas, USA) was used to analyse mRNA and protein expression in relation to disease, patient age of death, tissue post-mortem delay and gender. Where necessary, data was transformed to normality before performing regression analysis. For all tests, values of $p < 0.05$ were considered statistically significant.

Results

Cohort variances

The 49 AD cases used ranged from 54-98 y (mean = 81 y, SD = 9 y) and the 46 control cases used from 43-95y (mean = 79 y, SD = 11 y). In keeping with AD incidence, there was a higher proportion of female cases in the AD group (61.2%) compared with male (38.8%) and roughly an even gender split in control cases (female: 45.7%; male 54.3%). There was no significant difference in tissue post-mortem delay between AD (mean = 40 h, SD = 21 h) and control samples (mean = 43 h, SD = 38 h) (two-tailed Mann-Whitney; p=0.63; Table 1). Multiple regression analysis revealed a significant effect of post-mortem delay (PMD) on mRNA expression (Table 3). Specifically, NeuN mRNA expression correlated inversely with tissue post-mortem delay (n=47, Spearman r = -0.48, p=0.00). Subsequent analysis excluded cases with PMD >72 h. After exclusion, PMD still influenced NeuN mRNA expression (n=43, Spearman r = -0.45, p=0.00) but there was no effect of PMD on NeuN protein expression (n=76, Spearman r = -0.11, p=0.23). Therefore, KIF mRNA expression was normalised to an alternative neuronal house-keeping gene, neuron-specific enolase (ENO-2). There was no effect of PMD on ENO-2 mRNA expression (n=42, Spearman r = 0.26, p=0.09).

Upregulation of KIF genes in AD

There was a 4-fold increase in KIF5A mRNA relative to ENO-2 mRNA in AD compared to controls ($p < 0.001$; Figure 1A). There was also a 3-fold increase in KIF1B mRNA in AD cases ($p < 0.01$; Figure 1B). There was no significant difference in KIF21B mRNA expression between control and AD cases ($p = 0.32$; Figure 1C). Multi-regression analysis showed no effect of patient age of death, tissue post-mortem delay or gender on KIF mRNA expression, when normalised to ENO-2 (Table 3).

Elevated KIF5A, KIF1B and KIF21B protein in AD

Immuno dot-blot revealed significantly increased KIF5A protein in AD compared to control tissue, after adjustment for NeuN content ($p < 0.05$; Figure 2A). There were also significant increases in KIF1B ($p < 0.001$; Figure 2B) and KIF21B protein ($p < 0.001$; Figure 2C), after adjustment for NeuN. Multi-variate analysis showed no significant effect of tissue post-mortem delay or gender on KIF protein expression but there was a significant

effect of aging on KIF1B protein expression (Table 4). In order to establish whether increased KIF expression is an early event in AD pathogenesis, KIF expression was also sub-categorised according to Braak score, ranging from 0-6. One-way ANOVA with post-hoc Bonferroni did not reveal significant differences between the groups (Supplementary Table 1).

KIF5A protein correlates inversely with hyperphosphorylated tau in AD brains

As expected, we found a significant increase in hyperphosphorylated tau in AD compared to controls, adjusted for NeuN ($p < 0.001$; Figure 3). This was replicated in multi-variate analysis, however, there was a significant influence of patient age on tau expression ($p<0.05$, Table 4). Univariate analysis showed no correlation between KIF5A expression (adjusted for GAPDH [33]) and hyperphosphorylated tau (adjusted for NeuN) in control (Pearson r = -0.30, p=0.09) or AD cases (Spearman r -0.27, p=0.10; Table 5). Due to the influence of age, additional multi-variate analysis was performed which revealed a significant effect of KIF5A protein on hyperphosphorylated tau expression in AD cases (p=0.04, Table 6). Both univariate and multi-variate analysis showed no significant correlations between tau and KIF1B or KIF21B (Table 5 and Table 6).

KIF5A protein correlates inversely with AβPP and soluble Aβ in AD

AβPP protein level (adjusted for NeuN) was significantly elevated in AD tissue compared with control in univariate analysis ($p<0.05$; Figure 4A). However, this increase was not significant in subsequent multi-variate analysis, considering patient age of death, tissue PMD and gender (p=0.15, Table 4). There was a significant inverse correlation between KIF5A (adjusted for GAPDH) and AβPP protein level (adjusted for NeuN) in AD cases (Spearman r = -0.53, $p < 0.001$; Figure 4B) and control cases (Spearman r = -0.42, $p<0.05$; Table 5). As expected, there was a significant increase in insoluble Aβ levels in AD cases compared with control (two-tailed Mann-Whitney, $p < 0.001$), which was consolidated in multi-variate analysis (Table 4). There was no correlation between KIF5A expression and insoluble Aβ in AD cases (Pearson r = 0.05, p = -0.08; Table 5). Soluble Aβ was elevated in AD cases but not to significance (p = 0.06; Figure 4C), as verified in multi-variate analysis (p=0.05; Table 4). Like AβPP, soluble Aβ levels correlated inversely with KIF5A in AD cases (Pearson r = -0.49, $p < 0.05$; Figure 4D). Previous studies have suggested that the level of soluble Aβ tends to fall with increased deposition of insoluble Aβ [34, 35]. However, KIF5A level did not correlate with the ratio of soluble: insoluble Aβ in AD cases

(Spearman r = -0.35, p =0.09; Table 5). Univariate analysis showed no association between KIF21B or KIF1B with AβPP, soluble Aβ, insoluble Aβ and soluble:insoluble Aβ in control or AD cases (Table 5). Considering the effect of age on KIF1B expression, multi-variate analysis was also performed which showed no significant correlation between KIF1B and AβPP, soluble Aβ and insoluble Aβ, which was not affected by age (Supplementary Table 2).

Discussion

Dysregulated KIF expression has been investigated in relation to several neurodegenerative diseases but remains relatively little studied in AD [29, 36]. We have found increased KIF gene and protein expression in AD, and significant inverse correlations between KIF5A expression and AβPP and soluble Aβ in AD.

KIF5A exists predominantly as a tetramer comprising two dimerised kinesin heavy chains, and two kinesin light chains (KLC1 and KLC2) attached at the tail domain of the KHCs. Studies in mice have shown KIF5A knock-out is neonatal lethal and post-natal targeting of the gene results in reduced axon calibre, eventual axon loss and hind-limb paralysis [9]. KIF5A is believed to transport several cargoes through association with KLCs, including AβPP, phosphorylated NFs and SNARE complex components; SNAP-25 and syntaxin-1b [17]. It has been suggested that genetic variability in the KLC1 gene may influence the development of AD [20]. In mice, deletion of the KLC1 subunit leads to early selective defects of axonal transport of several cargoes including AβPP, NF and tau aggregates, causing cytoskeletal disorganisation [37].

We found increased KIF5A protein in AD to be associated with elevated levels of the corresponding transcript. It is possible that KIF5A is upregulated as an adaptive response in an attempt to clear or circumvent large protein aggregates within the neuron or to compensate for potential reduced activity of other motors. Elevated KIF5A mRNA has also been found in brain tissue from demented compared to non-demented patients with Parkinson's disease [38]. Univariate analysis showed a significant increase in AβPP levels in AD compared with control. However, this effect was lost in multi-variate analysis of the cohort, in keeping with previous studies [39, 40]. KIF5A protein levels correlated inversely with that of AβPP, as previously reported in MS white matter [13]. AβPP is a type I transmembrane protein with suspected roles in cell adhesion, regulation of gene expression, and iron export [41]. AβPP transport by KIF5A is thought to be mediated by KLC association with AβPP-containing vesicles [18]. The subcellular distribution of AβPP plays a critical role in its metabolism, including the cleavage

by β- and γ- secretases that generates pathogenic Aβ peptides [35, 42-52]. Maintenance of neuronal transport of AβPP by upregulation of KIF5A may help to maintain normal metabolism of AβPP (and thereby neuronal viability) for longer than would otherwise be the case. In support of this, although soluble Aβ levels were higher in AD than control tissue, the levels correlated inversely with that of KIF5A. KIF5A level was not related to the ratio of soluble: insoluble Aβ, suggesting that KIF5A does not significantly influence the deposition of Aβ. However, we hypothesise that upregulation of KIF5A may temporarily ameliorate the damaging effects of abnormal intracellular protein aggregates through maintained intraneuronal transport.

NFTs form through aggregation of hyperphosphorylated tau [53]. Multi-variate analysis of our cohort revealed levels of hyperphosphorylated tau declined with age. This is likely to be influenced by many confounding variables such as diet, genetics and lifestyle [54]. However, taking aging into account, we found KIF5A levels correlated inversely with hyperphosphorylated tau levels in AD cases. This again supports the hypothesis that KIF5A upregulation is crucial in maintaining intraneuronal transport. However, the effectiveness of KIF5A-mediated transport in AD still needs to be determined. Studies have reported that pathogenic forms of tau inhibit axonal transport through activation of the protein phosphatase 1/glycogen synthase kinase 3 (PP1/GSK3) pathway [55], which is believed to cause dissociation of KIF5A from its cargo through phosphorylation of KLC [29].

KIF1B mRNA and protein levels were higher in AD than control tissue. KIF1B has two splice variants, KIF1Bα and KIF1Bβ, which exist as KHC monomers. KIF1Bα transports mitochondria, synaptic scaffolding molecules (SCAM) and post-synaptic density (PSD) proteins PSD-95 and PSD-97. KIF1Bβ transports synaptic vesicle precursors including synaptotagmin, synaptophysin and SV2. In humans, a missense mutation in the KIF1Bβ gene is linked to CMT-2A [27], characterised clinically by weakness and atrophy of distal muscles, depressed or absent tendon reflexes and mild sensory loss. The kif1bβ mutation results in a glutamine to leucine substitution in the ATP-binding site of the kif1bβ motor domain, which causes a reduction in microtubule-ATPase activity and consequent reduction in the transport of cargoes. Impaired delivery of synaptic vesicle precursors to axons and nerve terminals contributes to progressive dysfunction of peripheral neurons [56]. Because of their overlapping cargoes, a level of functional redundancy is thought to exist between KIF1B and KIF5A. Campbell *et al* [15] studied functional redundancy of KIFs in zebrafish and found that kif1b overexpression cannot compensate for loss of kif5a-mediated mitochondrial transport but suggested a dual function in maintaining peripheral sensory neuronal function through the transport of non-mitochondrial cargoes. These non-mitochondrial cargoes are most likely to be synaptic proteins. Indeed, rodent studies have suggested alternative

roles for KIF5A and KIF1B in modulating mitochondrial motility, suggesting KIF1B overexpression reduces mitochondrial transport, whereas KIF5A overexpression increases motility [57]. We had considered the possibility that elevated KIF5A might partly be a physiological compensatory response to reduced KIF1B. We found both KIF5A and KIF1B to be elevated in AD, however, further investigation of family isoforms, in particular KIF1Bα and KIF1Bβ, could help elucidate potential subunit redundancy. The precise affinity of KIF5A for cargoes such as AβPP and the degree of functional redundancy between axonal motors from different sub-groups remains an open question [58].

The anterograde motor protein KIF21B was increased in AD compared with control tissue. KIF21B is enriched in the dendrites and transports γ2-subunit-containing GABAA receptor vesicles. Altered expression of KIF21B may be involved in the regulation of receptor density that mediates GABAergic synaptic plasticity [28]. Kreft *et al* [59] found that KIF21B mRNA was increased in early-onset AD ($\leq$ 62 y at the time of death) and that the level correlated with shorter disease duration, and increased disease severity as assessed by neuropathology. In our study, the elevation in KIF21B mRNA in AD was not statistically significant. However, the mean age at death in our AD cohort was 81 y, and Kreft *et al* did not find any increase in KIF21B mRNA in an older AD cohort ($\geq$ 72 y at death).

In summary, we have found upregulation of three KIFs in AD. It remains to be determined whether upregulation is an adaptive response that helps to maintain intraneuronal transport and stabilise axonal structure in AD or whether it contributes to neurodegeneration.

Acknowledgements

We thank the South West Dementia Brain Bank (SWDBB) for providing brain tissue for this study. The SWDBB is part of the Brains for Dementia Research program, jointly funded by Alzheimer's Research UK and the Alzheimer's Society, and is supported by BRACE (Bristol Research into Alzheimer's and Care of the Elderly) and the Medical Research Council.

Conflict of Interest

The authors have no conflict of interest to report.

References

[1] Hirokawa N, Niwa S, Tanaka Y (2010) Molecular motors in neurons: transport mechanisms and roles in brain function, development, and disease. *Neuron* **68**, 610-638.

[2] Hirokawa N, Noda Y (2008) Intracellular transport and kinesin superfamily proteins, KIFs: structure, function, and dynamics. *Physiol Rev* **88**, 1089-1118.

[3] Miki H, Setou M, Kaneshiro K, Hirokawa N (2001) All kinesin superfamily protein, KIF, genes in mouse and human. *Proc Natl Acad Sci U S A* **98**, 7004-7011.

[4] Brady ST (1985) A novel brain ATPase with properties expected for the fast axonal transport motor. *Nature* **317**, 73-75.

[5] Vale RD, Fletterick RJ (1997) The design plan of kinesin motors. *Annu Rev Cell Dev Biol* **13**, 745-777.

[6] Reid E, Kloos M, Ashley-Koch A, Hughes L, Bevan S, Svenson IK, Graham FL, Gaskell PC, Dearlove A, Pericak-Vance MA, Rubinsztein DC, Marchuk DA (2002) A kinesin heavy chain (KIF5A) mutation in hereditary spastic paraplegia (SPG10). *Am J Hum Genet* **71**, 1189-1194.

[7] Crimella C, Baschirotto C, Arnoldi A, Tonelli A, Tenderini E, Airoldi G, Martinuzzi A, Trabacca A, Losito L, Scarlato M, Benedetti S, Scarpini E, Spinicci G, Bresolin N, Bassi MT (2012) Mutations in the motor and stalk domains of KIF5A in spastic paraplegia type 10 and in axonal Charcot-Marie-Tooth type 2. *Clin Genet* **82**, 157-164.

[8] Kawaguchi K (2013) Role of kinesin-1 in the pathogenesis of SPG10, a rare form of hereditary spastic paraplegia. *Neuroscientist* **19**, 336-344.

[9] Xia CH, Roberts EA, Her LS, Liu X, Williams DS, Cleveland DW, Goldstein LS (2003) Abnormal neurofilament transport caused by targeted disruption of neuronal kinesin heavy chain KIF5A. *J Cell Biol* **161**, 55-66.

[10] Alcina A, Fedetz M, Fernandez O, Saiz A, Izquierdo G, Lucas M, Leyva L, Garcia-Leon JA, Abad-Grau Mdel M, Alloza I, Antiguedad A, Garcia-Barcina MJ, Vandenbroeck K, Varade J, de la Hera B, Arroyo R, Comabella M, Montalban X, Petit-Marty N, Navarro A, Otaegui D, Olascoaga J, Blanco Y, Urcelay E, Matesanz F (2013) Identification of a functional variant in the KIF5A-CYP27B1-METTL1-FAM119B locus associated with multiple sclerosis. *J Med Genet* **50**, 25-33.

[11] International Multiple Sclerosis Genetics C, Wellcome Trust Case Control C, Sawcer S, Hellenthal G, Pirinen M, Spencer CC, Patsopoulos NA, Moutsianas L, Dilthey A, Su Z, Freeman C, Hunt SE, Edkins S, Gray E, Booth DR, Potter SC, Goris A, Band G, Oturai AB, Strange A, Saarela J, Bellenguez C, Fontaine B, Gillman M, Hemmer B, Gwilliam R, Zipp F, Jayakumar A, Martin R, Leslie S, Hawkins S, Giannoulatou E, D'Alfonso S, Blackburn H, Martinelli Boneschi F, Liddle J, Harbo HF, Perez ML, Spurkland A, Waller MJ, Mycko MP, Ricketts M, Comabella M, Hammond N, Kockum I, McCann OT, Ban M, Whittaker P, Kemppinen A, Weston P, Hawkins C, Widaa S, Zajicek J, Dronov S, Robertson N, Bumpstead SJ, Barcellos LF, Ravindrarajah R, Abraham R, Alfredsson L, Ardlie K, Aubin C, Baker A, Baker K, Baranzini SE, Bergamaschi L, Bergamaschi R, Bernstein A, Berthele A, Boggild M, Bradfield JP, Brassat D, Broadley SA, Buck D, Butzkueven H, Capra R, Carroll WM, Cavalla P, Celius EG, Cepok S, Chiavacci R, Clerget-Darpoux F, Clysters K, Comi G, Cossburn M, Cournu-Rebeix I, Cox MB, Cozen W, Cree BA, Cross AH, Cusi D, Daly MJ, Davis E, de Bakker PI, Debouverie M, D'Hooghe M B, Dixon K, Dobosi R, Dubois B, Ellinghaus D, Elovaara I, Esposito F, Fontenille C, Foote S, Franke A, Galimberti D, Ghezzi A, Glessner J, Gomez R, Gout O, Graham C, Grant SF, Guerini FR, Hakonarson H, Hall P, Hamsten A, Hartung HP, Heard RN, Heath S, Hobart J, Hoshi M, Infante-Duarte C, Ingram G, Ingram W, Islam T, Jagodic M, Kabesch M, Kermode AG, Kilpatrick TJ, Kim C, Klopp N, Koivisto K, Larsson M, Lathrop M, Lechner-Scott JS, Leone MA, Leppa V, Liljedahl U, Bomfim IL, Lincoln RR, Link J, Liu J, Lorentzen AR, Lupoli S, Macciardi F, Mack T, Marriott M, Martinelli V, Mason D, McCauley JL, Mentch F, Mero IL, Mihalova T, Montalban X, Mottershead J, Myhr KM, Naldi P, Ollier W, Page A, Palotie A, Pelletier J, Piccio L, Pickersgill T, Piehl F, Pobywajlo S, Quach HL, Ramsay PP, Reunanen M, Reynolds R, Rioux JD, Rodegher M, Roesner S, Rubio JP, Ruckert IM, Salvetti M, Salvi E, Santaniello A, Schaefer CA, Schreiber S, Schulze C, Scott RJ, Sellebjerg F, Selmaj KW, Sexton D, Shen L, Simms-Acuna B, Skidmore S, Sleiman PM, Smestad C, Sorensen PS, Sondergaard HB, Stankovich J, Strange RC, Sulonen AM, Sundqvist E, Syvanen AC, Taddeo F, Taylor B, Blackwell JM, Tienari P, Bramon E, Tourbah A, Brown MA, Tronczynska E, Casas JP, Tubridy N, Corvin A, Vickery J, Jankowski J, Villoslada P, Markus HS, Wang K, Mathew CG, Wason J, Palmer CN, Wichmann HE, Plomin R, Willoughby E, Rautanen A, Winkelmann J, Wittig M, Trembath RC, Yaouanq J, Viswanathan AC, Zhang H, Wood NW, Zuvich R, Deloukas P, Langford C, Duncanson A, Oksenberg JR, Pericak-Vance MA, Haines JL, Olsson T, Hillert J, Ivinson AJ, De Jager PL, Peltonen L, Stewart GJ, Hafler DA, Hauser SL, McVean G, Donnelly P, Compston A (2011) Genetic risk and a primary role for cell-mediated immune mechanisms in multiple sclerosis. *Nature* **476**, 214-219.

[12] Hares K, Kemp K, Rice C, Gray E, Scolding N, Wilkins A (2014) Reduced axonal motor protein expression in non-lesional grey matter in multiple sclerosis. *Mult Scler* **20**, 812-821.
[13] Hares K, Redondo J, Kemp K, Rice C, Scolding N, Wilkins A (2017) Axonal motor protein KIF5A and associated cargo deficits in multiple sclerosis lesional and normal-appearing white matter. *Neuropathol Appl Neurobiol* **43**, 227-241.
[14] Hirokawa N, Noda Y, Tanaka Y, Niwa S (2009) Kinesin superfamily motor proteins and intracellular transport. *Nat Rev Mol Cell Biol* **10**, 682-696.
[15] Campbell PD, Shen K, Sapio MR, Glenn TD, Talbot WS, Marlow FL (2014) Unique function of Kinesin Kif5A in localization of mitochondria in axons. *J Neurosci* **34**, 14717-14732.
[16] Randall TS, Moores C, Stephenson FA (2013) Delineation of the TRAK binding regions of the kinesin-1 motor proteins. *FEBS Lett* **587**, 3763-3769.
[17] Szodorai A, Kuan YH, Hunzelmann S, Engel U, Sakane A, Sasaki T, Takai Y, Kirsch J, Muller U, Beyreuther K, Brady S, Morfini G, Kins S (2009) APP anterograde transport requires Rab3A GTPase activity for assembly of the transport vesicle. *J Neurosci* **29**, 14534-14544.
[18] Kamal A, Stokin GB, Yang Z, Xia CH, Goldstein LS (2000) Axonal transport of amyloid precursor protein is mediated by direct binding to the kinesin light chain subunit of kinesin-I. *Neuron* **28**, 449-459.
[19] Dhaenens CM, Van Brussel E, Schraen-Maschke S, Pasquier F, Delacourte A, Sablonniere B (2004) Association study of three polymorphisms of kinesin light-chain 1 gene with Alzheimer's disease. *Neurosci Lett* **368**, 290-292.
[20] Andersson ME, Sjolander A, Andreasen N, Minthon L, Hansson O, Bogdanovic N, Jern C, Jood K, Wallin A, Blennow K, Zetterberg H (2007) Kinesin gene variability may affect tau phosphorylation in early Alzheimer's disease. *Int J Mol Med* **20**, 233-239.
[21] Stokin GB, Lillo C, Falzone TL, Brusch RG, Rockenstein E, Mount SL, Raman R, Davies P, Masliah E, Williams DS, Goldstein LS (2005) Axonopathy and transport deficits early in the pathogenesis of Alzheimer's disease. *Science* **307**, 1282-1288.
[22] Pigino G, Morfini G, Pelsman A, Mattson MP, Brady ST, Busciglio J (2003) Alzheimer's presenilin 1 mutations impair kinesin-based axonal transport. *J Neurosci* **23**, 4499-4508.
[23] Pigino G, Pelsman A, Mori H, Busciglio J (2001) Presenilin-1 mutations reduce cytoskeletal association, deregulate neurite growth, and potentiate neuronal dystrophy and tau phosphorylation. *J Neurosci* **21**, 834-842.
[24] Cleveland DW, Hwo SY, Kirschner MW (1977) Purification of tau, a microtubule-associated protein that induces assembly of microtubules from purified tubulin. *J Mol Biol* **116**, 207-225.
[25] Aulchenko YS, Hoppenbrouwers IA, Ramagopalan SV, Broer L, Jafari N, Hillert J, Link J, Lundstrom W, Greiner E, Dessa Sadovnick A, Goossens D, Van Broeckhoven C, Del-Favero J, Ebers GC, Oostra BA, van Duijn CM, Hintzen RQ (2008) Genetic variation in the KIF1B locus influences susceptibility to multiple sclerosis. *Nat Genet* **40**, 1402-1403.
[26] Goris A, Boonen S, D'Hooghe M B, Dubois B (2010) Replication of KIF21B as a susceptibility locus for multiple sclerosis. *J Med Genet* **47**, 775-776.
[27] Ben Othmane K, Middleton LT, Loprest LJ, Wilkinson KM, Lennon F, Rozear MP, Stajich JM, Gaskell PC, Roses AD, Pericak-Vance MA, et al. (1993) Localization of a gene (CMT2A) for autosomal dominant Charcot-Marie-Tooth disease type 2 to chromosome 1p and evidence of genetic heterogeneity. *Genomics* **17**, 370-375.
[28] Labonte D, Thies E, Kneussel M (2014) The kinesin KIF21B participates in the cell surface delivery of gamma2 subunit-containing GABAA receptors. *Eur J Cell Biol* **93**, 338-346.
[29] Kanaan NM, Pigino GF, Brady ST, Lazarov O, Binder LI, Morfini GA (2013) Axonal degeneration in Alzheimer's disease: when signaling abnormalities meet the axonal transport system. *Exp Neurol* **246**, 44-53.
[30] Montine TJ, Phelps CH, Beach TG, Bigio EH, Cairns NJ, Dickson DW, Duyckaerts C, Frosch MP, Masliah E, Mirra SS, Nelson PT, Schneider JA, Thal DR, Trojanowski JQ, Vinters HV, Hyman BT, National Institute on A, Alzheimer's A (2012) National Institute on Aging-Alzheimer's Association guidelines for the neuropathologic assessment of Alzheimer's disease: a practical approach. *Acta Neuropathol* **123**, 1-11.
[31] Glennon EB, Whitehouse IJ, Miners JS, Kehoe PG, Love S, Kellett KA, Hooper NM (2013) BIN1 is decreased in sporadic but not familial Alzheimer's disease or in aging. *PLoS One* **8**, e78806.
[32] van Helmond Z, Miners JS, Kehoe PG, Love S (2010) Oligomeric Abeta in Alzheimer's disease: relationship to plaque and tangle pathology, APOE genotype and cerebral amyloid angiopathy. *Brain Pathol* **20**, 468-480.
[33] Kim JH (1999) Spurious correlation between ratios with a common divisor. *Statistics & Probability Letters* **44**, 383-386.

[34] van Helmond Z, Miners JS, Kehoe PG, Love S (2010) Higher soluble amyloid beta concentration in frontal cortex of young adults than in normal elderly or Alzheimer's disease. *Brain Pathol* **20**, 787-793.
[35] Miners JS, Jones R, Love S (2014) Differential changes in Abeta42 and Abeta40 with age. *J Alzheimers Dis* **40**, 727-735.
[36] Millecamps S, Julien JP (2013) Axonal transport deficits and neurodegenerative diseases. *Nat Rev Neurosci* **14**, 161-176.
[37] Falzone TL, Stokin GB, Lillo C, Rodrigues EM, Westerman EL, Williams DS, Goldstein LS (2009) Axonal stress kinase activation and tau misbehavior induced by kinesin-1 transport defects. *J Neurosci* **29**, 5758-5767.
[38] Stamper C, Siegel A, Liang WS, Pearson JV, Stephan DA, Shill H, Connor D, Caviness JN, Sabbagh M, Beach TG, Adler CH, Dunckley T (2008) Neuronal gene expression correlates of Parkinson's disease with dementia. *Mov Disord* **23**, 1588-1595.
[39] Holtzman DM, Mobley WC (1991) Molecular studies in Alzheimer's disease. *Trends Biochem Sci* **16**, 140-144.
[40] Rumble B, Retallack R, Hilbich C, Simms G, Multhaup G, Martins R, Hockey A, Montgomery P, Beyreuther K, Masters CL (1989) Amyloid A4 protein and its precursor in Down's syndrome and Alzheimer's disease. *N Engl J Med* **320**, 1446-1452.
[41] Zheng H, Koo EH (2011) Biology and pathophysiology of the amyloid precursor protein. *Mol Neurodegener* **6**, 27.
[42] Rajendran L, Annaert W (2012) Membrane trafficking pathways in Alzheimer's disease. *Traffic* **13**, 759-770.
[43] Zhang YW, Thompson R, Zhang H, Xu H (2011) APP processing in Alzheimer's disease. *Mol Brain* **4**, 3.
[44] Furukawa K, Sopher BL, Rydel RE, Begley JG, Pham DG, Martin GM, Fox M, Mattson MP (1996) Increased activity-regulating and neuroprotective efficacy of alpha-secretase-derived secreted amyloid precursor protein conferred by a C-terminal heparin-binding domain. *J Neurochem* **67**, 1882-1896.
[45] Mattson MP (1997) Cellular actions of beta-amyloid precursor protein and its soluble and fibrillogenic derivatives. *Physiol Rev* **77**, 1081-1132.
[46] Maclean CJ, Baker HF, Ridley RM, Mori H (2000) Naturally occurring and experimentally induced beta-amyloid deposits in the brains of marmosets (Callithrix jacchus). *J Neural Transm (Vienna)* **107**, 799-814.
[47] Wang J, Dickson DW, Trojanowski JQ, Lee VM (1999) The levels of soluble versus insoluble brain Abeta distinguish Alzheimer's disease from normal and pathologic aging. *Exp Neurol* **158**, 328-337.
[48] Lue LF, Kuo YM, Roher AE, Brachova L, Shen Y, Sue L, Beach T, Kurth JH, Rydel RE, Rogers J (1999) Soluble amyloid beta peptide concentration as a predictor of synaptic change in Alzheimer's disease. *Am J Pathol* **155**, 853-862.
[49] Gong Y, Chang L, Viola KL, Lacor PN, Lambert MP, Finch CE, Krafft GA, Klein WL (2003) Alzheimer's disease-affected brain: presence of oligomeric A beta ligands (ADDLs) suggests a molecular basis for reversible memory loss. *Proc Natl Acad Sci U S A* **100**, 10417-10422.
[50] Dahlgren KN, Manelli AM, Stine WB, Jr., Baker LK, Krafft GA, LaDu MJ (2002) Oligomeric and fibrillar species of amyloid-beta peptides differentially affect neuronal viability. *J Biol Chem* **277**, 32046-32053.
[51] Lesne S, Koh MT, Kotilinek L, Kayed R, Glabe CG, Yang A, Gallagher M, Ashe KH (2006) A specific amyloid-beta protein assembly in the brain impairs memory. *Nature* **440**, 352-357.
[52] Shankar GM, Li S, Mehta TH, Garcia-Munoz A, Shepardson NE, Smith I, Brett FM, Farrell MA, Rowan MJ, Lemere CA, Regan CM, Walsh DM, Sabatini BL, Selkoe DJ (2008) Amyloid-beta protein dimers isolated directly from Alzheimer's brains impair synaptic plasticity and memory. *Nat Med* **14**, 837-842.
[53] Iqbal K, Liu F, Gong CX, Alonso Adel C, Grundke-Iqbal I (2009) Mechanisms of tau-induced neurodegeneration. *Acta Neuropathol* **118**, 53-69.
[54] Granzotto A, Zatta P (2014) Resveratrol and Alzheimer's disease: message in a bottle on red wine and cognition. *Front Aging Neurosci* **6**, 95.
[55] Kanaan NM, Morfini GA, LaPointe NE, Pigino GF, Patterson KR, Song Y, Andreadis A, Fu Y, Brady ST, Binder LI (2011) Pathogenic forms of tau inhibit kinesin-dependent axonal transport through a mechanism involving activation of axonal phosphotransferases. *J Neurosci* **31**, 9858-9868.
[56] Zhao C, Takita J, Tanaka Y, Setou M, Nakagawa T, Takeda S, Yang HW, Terada S, Nakata T, Takei Y, Saito M, Tsuji S, Hayashi Y, Hirokawa N (2001) Charcot-Marie-Tooth disease type 2A caused by mutation in a microtubule motor KIF1Bbeta. *Cell* **105**, 587-597.
[57] Melo TQ, D'Unhao A M, Martins SA, Farizatto KL, Chaves RS, Ferrari MF (2013) Rotenone-dependent changes of anterograde motor protein expression and mitochondrial mobility in brain areas related to neurodegenerative diseases. *Cell Mol Neurobiol* **33**, 327-335.

[58] Morfini G, Schmidt N, Weissmann C, Pigino G, Kins S (2016) Conventional kinesin: Biochemical heterogeneity and functional implications in health and disease. *Brain Res Bull* **126**, 347-353.
[59] Kreft KL, van Meurs M, Wierenga-Wolf AF, Melief MJ, van Strien ME, Hol EM, Oostra BA, Laman JD, Hintzen RQ (2014) Abundant kif21b is associated with accelerated progression in neurodegenerative diseases. *Acta Neuropathol Commun* **2**, 144.

Tables

Table 1. Clinical characteristics of Alzheimer's disease and control patient cohort.

Patient ID	Age (yrs)	Sex (M/F)	Post-mortem delay (hrs)	Braak stage	Patient ID	Age (yrs)	Sex (M/F)	Post-mortem delay (hrs)	Braak stage
AD 1	89	F	71	5	**C 1**	62	M	4	0
AD 2	78	F	77	6	**C 2**	95	F	46	0
AD 3	78	F	9	5	**C 3**	78	F	24	2
AD 4	81	F	42	6	**C 4**	83	M	80	3
AD 5	91	F	37	4	**C5**	64	M	12	2
AD 6	77	F	43	4	**C 6**	64	M	16	0
AD 7	96	F	53	4	**C 7**	80	M	106	2
AD 8	87	F	72	5	**C 8**	90	M	45	2
AD 9	87	F	67	5	**C 9**	81	F	103	2
AD 10	79	F	70	3	**C 10**	64	M	23	2
AD 11	81	M	29	4	**C 11**	77	M	55	1
AD 12	91	F	70	5	**C 12**	80	M	12	2
AD 13	78	F	35	6	**C 13**	73	M	36	2
AD 14	83	F	43	5	**C 14**	88	F	62	2
AD 15	70	F	25	6	**C 15**	88	F	72	0
AD 16	78	F	4	5	**C 16**	93	F	18	2
AD 17	69	M	48	5	**C 17**	80	F	92	0
AD 18	74	M	50	5	**C 18**	88	F	28	2
AD 19	80	F	21	5	**C 19**	82	M	30	2
AD 20	95	M	48	3	**C 20**	84	M	48	3
AD 21	89	F	4	6	**C 21**	90	M	48	2
AD 22	79	M	28	6	**C 22**	75	M	48	2
AD 23	85	M	66	6	**C 23**	89	F	15	2
AD 24	95	F	74	3	**C 24**	73	M	33	1
AD 25	81	F	66	4	**C 25**	69	M	66	2
AD 26	80	M	31	6	**C 26**	73	F	59	1
AD 27	90	F	21	4	**C 27**	83	F	24	2
AD 28	57	F	24	5	**C 28**	82	M	3	2
AD 29	54	F	24	6	**C 29**	79	M	24	-
AD 30	84	F	20	5	**C 30**	43	F	12	-
AD 31	78	M	21	3	**C 31**	76	F	12	-
AD 32	93	M	20	6	**C 32**	84	F	17	1

AD 33	80	M	5	6	**C 33**	82	F	37	2
AD 34	87	F	55	5	**C 34**	72	F	24	0
AD 35	74	M	24	5	**C 35**	78	M	48	1
AD 36	89	F	39	5	**C 36**	81	M	3	2
AD 37	84	M	64	5	**C 37**	82	M	56	2
AD 38	73	F	38	5	**C 38**	76	M	23	2
AD 39	68	M	61	6	**C 39**	91	F	60	2
AD 40	83	M	48	5	**C 40**	82	F	96	3
AD 41	74	M	48	5	**C 41**	77	M	10	3
AD 42	78	M	49	6	**C 42**	75	M	6	3
AD 43	78	M	50	6	**C 43**	48	F	79	4
AD 44	85	M	50	6	**C 44**	93	F	53	3
AD 45	98	F	21	5	**C 45**	84	F	216	2
AD 46	83	F	32	6	**C 46**	90	M	6	2
AD 47	69	M	12	5					
AD 48	87	F	28	6					
AD 49	84	F	21	6					
Mean	**81 (+/- 9)**	**-**	**40 (+/- 21)**	**-**	**Mean**	**79 (+/- 11)**	**-**	**43 (+/- 38)**	**-**

Cases highlighted in red (post-mortem delay >72hrs) were removed from statistical analysis. Abbreviations: AD: Alzheimer's disease; C: control; F: female; Hrs: hours; M: male; Yrs: years.

Table 2. Antibodies used for immunoblotting.

Antigen	Species	Blocking Antibody	WB/DB Concentration	Product Code	Company
AβPP	Mouse	5% milk/TBS-Tween	1:2000	13-0200	Zymed
GAPDH	Mouse	5% BSA/TBS-Tween	1:10,000	Ab9484	Abcam
PHF-TAU	Mouse	5% BSA/TBS-Tween	1:500	MN1020	Thermoscientific
KIF5A	Rabbit	5% milk/TBS-Tween	1:1000	HPA004469	Sigma-Aldrich
KIF21B	Rabbit	5% milk/TBS-Tween	1:1000	HPA027274	Sigma-Aldrich
KIF1B	Rabbit	5% milk/TBS-Tween	1:500	A301-055A	Bethyl Labs
NeuN	Rabbit	5% milk/TBS-Tween	1:5000	Ab177487	Abcam

Abbreviations: AβPP: amyloid β protein precursor; BSA: Bovine serum albumin; DB: dot-blotting; KIF: kinesin superfamily protein; NeuN: neuronal nuclei; PHF: paired-helical filament; TBS: Tris-buffered saline; WB: western blotting.

Table 3. Multiple regression analysis of cohort variables on KIF mRNA expression

Sample type	n	Variables	Coefficient	Standard error	t	p value	95% Confidence intervals	
KIF5A to NeuN	44	***Treatment group***	1.12	0.39	2.85	0.01	0.32	1.92
		Age at death	0.03	0.03	0.96	0.35	-0.04	0.10
		Post-mortem delay	0.02	0.01	2.29	0.03	0.00	0.04
		Gender	-0.11	0.48	-0.22	0.83	-1.08	0.87
KIF1B to NeuN	46	***Treatment group***	1.22	0.45	2.71	0.01	0.31	2.13
		Age at death	-0.01	0.02	-0.43	0.67	-0.06	0.04
		Post-mortem delay	0.03	0.01	3.09	0.00	0.01	0.05
		Gender	0.64	0.46	1.39	0.17	-0.29	1.58
KIF21B to NeuN	45	***Treatment group***	0.13	0.09	1.38	0.18	-0.06	0.32
		Age at death	0.01	0.01	1.40	0.17	-0.00	0.00
		Post-mortem delay	-0.00	0.00	-0.36	0.72	-0.15	0.28
		Gender	0.07	0.11	0.63	0.53	-0.90	1.42
KIF5A to ENO-2	45	***Treatment group***	1.43	0.31	4.54	0.00	0.79	2.06
		Age at death	-0.04	0.02	-2.00	0.05	-0.07	0.00
		Post-mortem delay	-0.00	0.01	-0.21	0.84	-0.02	0.02
		Gender	0.05	0.35	0.13	0.89	-0.65	0.74
KIF1B to ENO-2	44	***Treatment group***	0.95	0.33	2.86	0.01	0.28	1.63
		Age at death	-0.04	0.02	-2.04	0.05	-0.08	-0.00
		Post-mortem delay	-0.00	0.01	-0.25	0.80	-0.02	0.01
		Gender	-0.16	0.34	-0.46	0.64	-0.85	0.53
KIF21B to ENO-2	45	***Treatment group***	0.59	0.61	0.97	0.34	-0.64	1.81
		Age at death	-0.03	0.04	-0.76	0.46	-0.12	0.05
		Post-mortem delay	-0.03	0.02	-1.75	0.09	-0.06	0.00
		Gender	-0.27	0.68	-0.40	0.69	-1.64	1.10

Significant correlations highlighted in red. Abbreviations: ENO-2: enolase-2; KIF: kinesin superfamily protein; NeuN: neuronal nuclei.

Table 4. Multiple regression analysis of cohort variables on protein expression

Sample type	n	Variables	Coefficient	Standard error	t	p value	95% Confidence intervals	
KIF5A	64	***Treatment group***	-0.53	0.14	-3.87	0.00	-0.80	-0.26
		Age at death	-0.01	0.01	-1.64	0.11	-0.03	0.00
		Post-mortem delay	0.00	0.00	1.15	0.25	-0.00	0.01
		Gender	0.03	0.14	0.19	0.85	-0.25	0.31
KIF1B	80	***Treatment group***	1.01	0.21	4.91	0.00	0.60	1.42
		Age at death	-0.03	0.01	-2.80	0.01	-0.05	-0.01
		Post-mortem delay	0.01	0.00	1.91	0.06	-0.00	0.02
		Gender	0.11	0.21	0.53	0.60	-0.31	0.54
KIF21B	75	***Treatment group***	0.53	0.15	3.62	0.00	0.24	0.81
		Age at death	-0.01	0.01	-0.98	0.33	-0.03	0.01
		Post-mortem delay	0.00	0.00	0.90	0.37	-0.00	0.01
		Gender	0.02	0.16	0.12	0.91	-0.29	0.33
AβPP	81	***Treatment group***	1.40	0.95	1.46	0.15	-0.50	3.30
		Age at death	-0.08	0.05	-1.42	0.16	-0.18	0.03
		Post-mortem delay	0.04	0.02	1.73	0.09	-0.01	0.09
		Gender	0.73	0.98	0.75	0.46	-1.22	2.69
PHF-Tau	77	***Treatment group***	-0.16	0.02	-8.32	0.00	-0.19	-0.12
		Age at death	0.00	0.00	2.07	0.04	0.00	0.00
		Post-mortem delay	-0.00	0.00	-1.42	0.16	-0.00	0.00
		Gender	-0.03	0.02	-1.28	0.21	-0.07	0.01
Insoluble Aβ	68	***Treatment group***	128.70	15.87	8.11	0.00	96.99	160.42
		Age at death	0.61	0.69	0.89	0.38	-0.76	1.99
		Post-mortem delay	-0.04	0.50	-0.09	0.93	-1.04	0.95
		Gender	-1.91	17.03	-0.11	0.91	-35.93	32.12
Soluble Aβ	63	***Treatment group***	0.35	0.17	2.04	0.05	0.01	0.69
		Age at death	0.01	0.01	0.89	0.38	-0.01	0.02
		Post-mortem delay	-0.01	0.00	-1.92	0.06	-0.02	0.00
		Gender	0.15	0.16	0.89	0.38	-0.18	0.47

Significant correlations highlighted in red. Abbreviations: : Aβ: amyloid β; AD: Alzheimer's disease, AβPP: amyloid β protein precursor; PHF: paired-helical filament; KIF: kinesin superfamily protein.

Table 5. Correlation analysis of kinesin superfamily protein with proteins linked to Alzheimer's disease.

Motor protein	Cargo protein	Sample	n	Correlation coefficient (r)	Significance (p)
KIF5A	*AβPP*	Control	33	-0.42	0.02
		AD	41	-0.53	0.00
	PHF-Tau	Control	32	-0.34	0.09
		AD	42	-0.27	0.10
	Insoluble Aβ	Control	24	-0.08	0.70
		AD	26	0.05	0.81
	Soluble Aβ	Control	20	-0.15	0.52
		AD	24	-0.49	0.02
	Soluble: Insoluble Aβ	Control	18	0.10	0.69
		AD	24	-0.35	0.09
KIF1B	*AβPP*	Control	32	-0.17	0.36
		AD	40	-0.18	0.26
	PHF-Tau	Control	31	0.09	0.63
		AD	38	0.23	0.16
	Insoluble Aβ	Control	22	-0.28	0.21
		AD	38	0.10	0.57
	Soluble Aβ	Control	17	0.15	0.58
		AD	34	-0.16	0.37
	Soluble: Insoluble Aβ	Control	17	0.21	0.43
		AD	37	-0.19	0.27
KIF21B	*AβPP*	Control	33	-0.30	0.09
		AD	43	-0.15	0.34
	PHF-Tau	Control	32	-0.30	0.10
		AD	40	-0.07	0.66
	Insoluble Aβ	Control	25	-0.15	0.49
		AD	40	-0.10	0.54
	Soluble Aβ	Control	19	-0.09	0.73
		AD	36	-0.09	0.61
	Soluble: Insoluble Aβ	Control	19	0.05	0.85
		AD	38	0.11	0.53

Significant correlations highlighted in red. Aβ: amyloid-β; AD: Alzheimer's disease, AβPP: amyloid β protein precursor; KIF: kinesin superfamily motor protein; PHF: paired-helical filament.

Table 6. Multiple regression analysis of KIF, age and tau protein expression

KIF protein	Sample type	n	Variables	Coefficient	Standard error	t	p value	95% Confidence intervals	
KIF5A	**Control**	32	***Age at death***	-0.73	0.95	-0.77	0.45	-2.67	1.22
			PHF-Tau	-34.13	23.36	-1.46	0.16	-81.91	13.64
	AD	39	***Age at death***	-0.01	0.02	-0.78	0.44	-0.05	0.02
			PHF-Tau	-0.00	0.00	-2.14	0.04	-0.00	-0.00
KIF1B	**Control**	31	***Age at death***	-0.81	0.56	-1.45	0.16	-1.95	0.33
			PHF-Tau	11.70	9.51	1.23	0.23	-7.78	31.18
	AD	38	***Age at death***	-1.61	1.73	-0.93	0.36	-5.12	1.91
			PHF-Tau	0.02	0.04	0.56	0.58	-0.06	0.11
KIF21B	**Control**	32	***Age at death***	0.22	0.43	0.51	0.61	-0.66	1.10
			PHF-Tau	-13.19	8.49	-1.55	0.13	-30.55	4.17
	AD	40	***Age at death***	-0.02	0.02	-1.27	0.21	-0.05	0.01
			PHF-Tau	-0.00	0.00	-1.00	0.32	-0.00	0.00

Significant correlations highlighted in red. AD: Alzheimer's disease, KIF: kinesin superfamily motor protein; PHF: paired-helical filament.

Figures legends/Figures

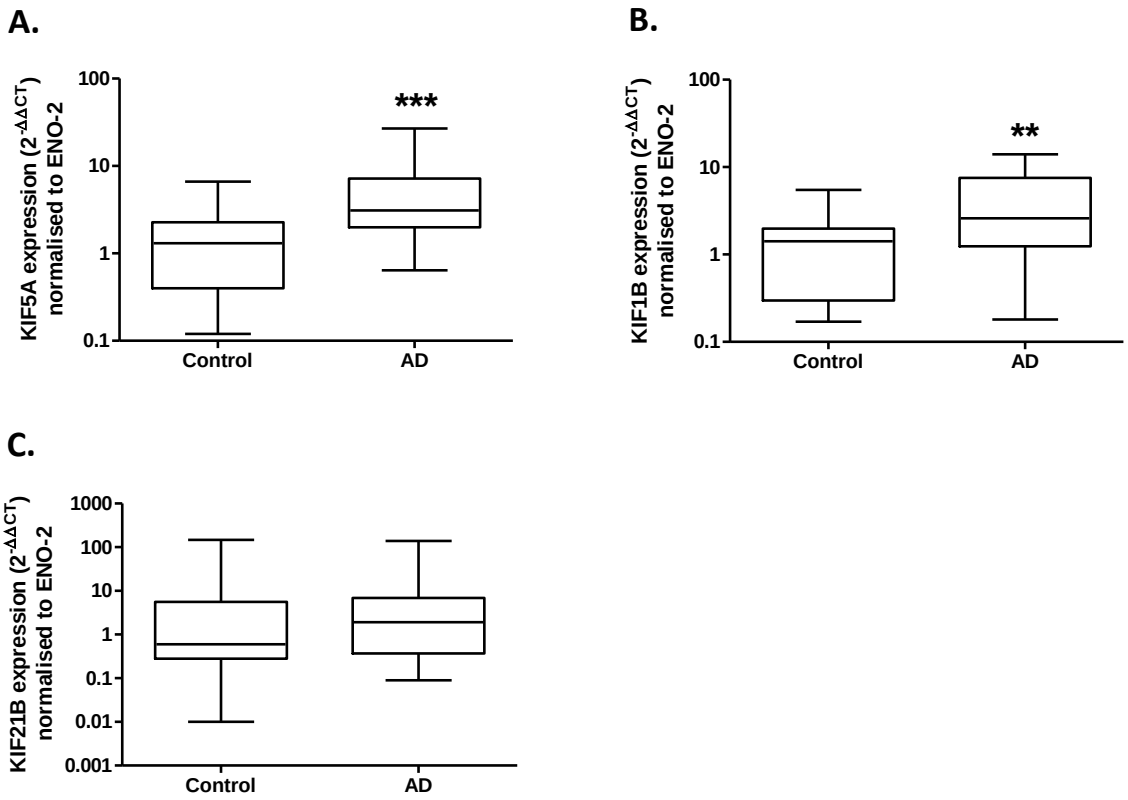

Figure 1. Upregulated gene expression of anterograde kinesin motors in Alzheimer's disease: quantitative real-time PCR performed with cDNA samples obtained from homogenised brain frontal lobe sections show a significant increase in KIF5A mRNA expression in AD cases (n=23) compared to control (n=22), when normalised to ENO-2 (A). KIF1B mRNA expression is significantly increased in AD cases (n=23) compared with control (n=22), when normalised to ENO-2 (B). KIF21B mRNA expression is not significantly different between control (n=21) and AD cases (n=23), when normalised to ENO-2 (C). Results expressed as median, IQR and min/max quartile. Statistical test used: two-tailed Mann-Whitney; **p<0.01, ***p<0.001. AD: Alzheimer's disease, IQR: inter-quartile range, KIF: kinesin superfamily protein, ENO-2: enolase-2.

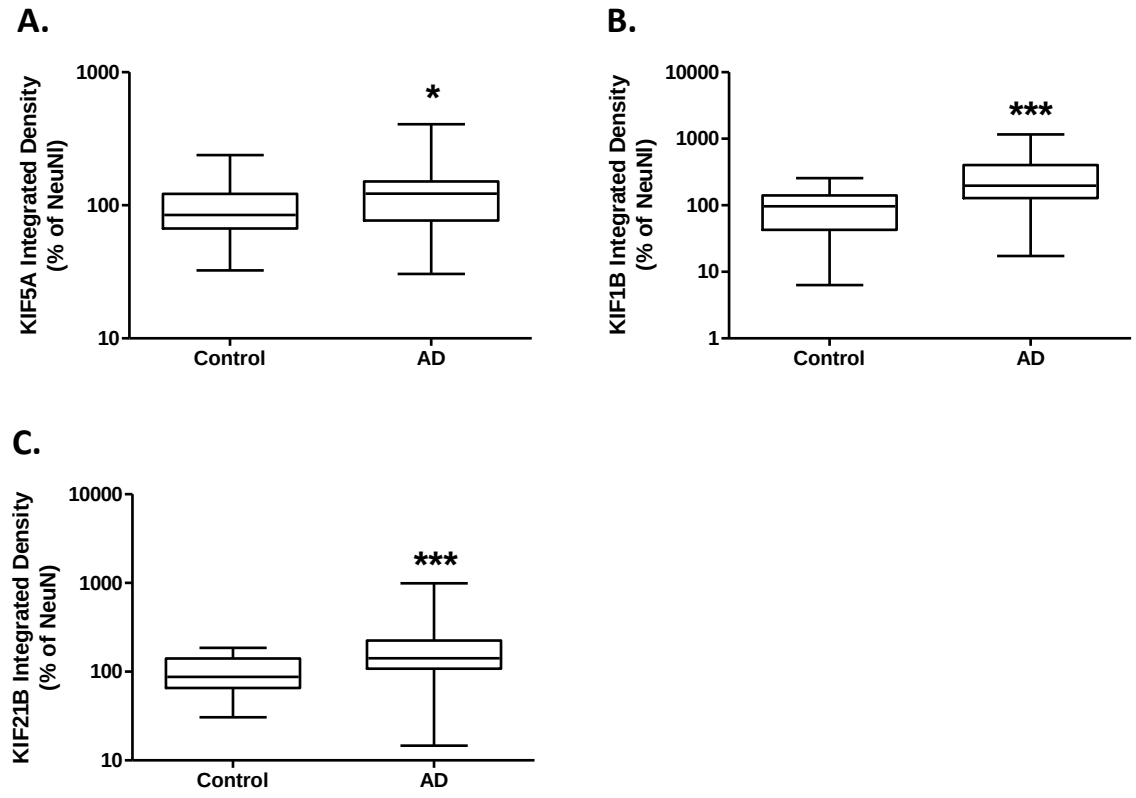

Figure 2. Increased anterograde kinesin motor protein expression in Alzheimer's disease: Protein levels derived from immuno dot-blot show a significant increase in anterograde kinesin motor protein KIF5A expression in AD cases (n=43), compared with control (n=35), when normalised to NeuN (A). KIF1B protein expression is significantly increased in AD cases (n=42), compared with control (n=33), when normalised to NeuN (B). KIF21B protein expression is significantly increased in AD cases (n=44), compared with control (n=36), when normalised to NeuN (C). Results expressed as median, IQR and min/max quartile. Statistical test used: two-tailed Mann-Whitney; *$p<0.05$, ***$p<0.001$. AD: Alzheimer's disease, IQR: inter-quartile range, KIF: kinesin superfamily protein, NeuN: neuronal nuclei.

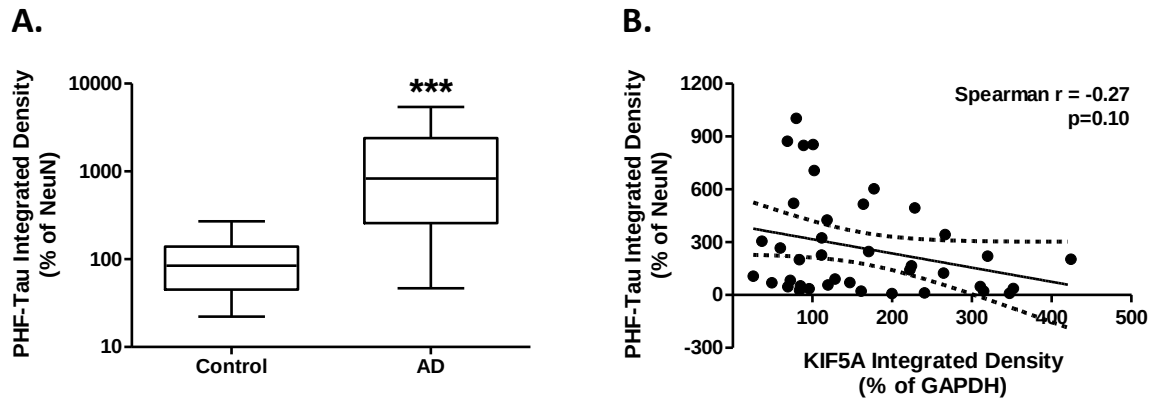

Figure 3. Elevated hyperphosphorylated tau protein expression in AD cases. Protein levels derived from immuno dot-blot show a significant increase in PHF-tau expression in AD cases (n=42) compared with control (n=35), when normalised to NeuN (A). Univariate analysis shows no significant correlation between KIF5A and PHF-Tau levels in AD cases (n=42; B). Results expressed as median, IQR and min/max quartile. Statistical test used: two-tailed Mann-Whitney (A). Correlation represented as line of best fit +/- 95% CI (B). ***p<0.001. AD: Alzheimer's disease, CI: confidence interval, IQR: inter-quartile range, KIF: kinesin superfamily motor protein, NeuN: neuronal nuclei, PHF: paired helical filament.

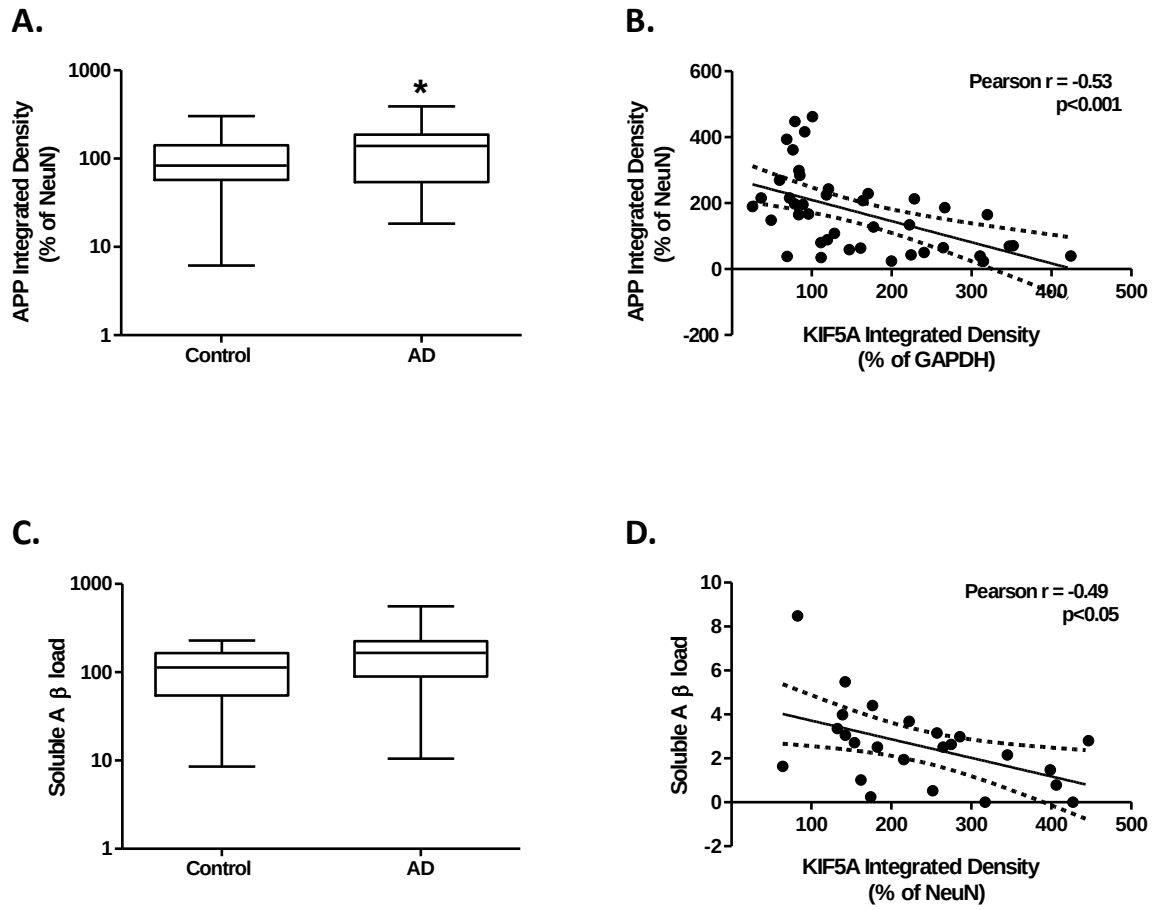

Figure 4. Higher kinesin motor KIF5A protein levels correlate with lower levels of amyloid precursor protein and soluble Aβ in AD. Protein levels derived from immuno dot-blot show a significant increase in AβPP expression in AD cases (n=45) compared with control (n=36), when normalised to NeuN (A). Significant inverse correlation between KIF5A protein levels normalised to GAPDH and AβPP protein levels, normalised to NeuN in AD (n=41; B). Protein levels obtained via ELISA show no significant difference in soluble Aβ protein expression in AD cases (n=42) compared with control (n=22; C). Significant inverse correlation between KIF5A protein levels normalised to NeuN and soluble Aβ protein levels in AD (n=24; D). Results expressed as median, IQR and min/max quartile. Statistical test used: two-tailed Mann-Whitney (A and C). Correlations represented as line of best fit +/- 95% CI (B and D). *p<0.05, ** p<0.01, ***p<0.001. Aβ: amyloid-β, AD: Alzheimer's disease, AβPP: amyloid β protein precursor, CI: confidence intervals, IQR: inter-quartile range, KIF: kinesin superfamily protein, NeuN: neuronal nuclei.

Supplementary Table 1. Analysis of Braak score on KIF expression using one-way ANOVA.

Bonferroni's Multiple Comparison Test	Mean difference	t	Significant? p<0.05?	Summary	95% CI of difference	
KIF5A						
0 vs 1	27.01	0.14	No	ns	-576.0	630.1
0 vs 2	-62.43	0.42	No	ns	-531.2	406.3
0 vs 3	-43.38	0.26	No	ns	-565.6	478.9
0 vs 4	52.38	0.29	No	ns	-524.6	630.2
0 vs 5	-141.50	0.93	No	ns	-618.2	335.3
0 vs 6	-133.60	0.87	No	ns	-615.6	348.4
1 vs 2	-89.45	0.60	No	ns	-558.2	-379.3
1 vs 3	-70.39	0.42	No	ns	-592.7	451.9
1 vs 4	25.81	0.14	No	ns	-551.6	603.2
1 vs 5	-168.50	1.11	No	ns	-645.2	308.3
1 vs 6	-160.60	1.05	No	ns	-642.7	321.4
2 vs 3	19.05	0.17	No	ns	-339.8	377.9
2 vs 4	115.30	0.83	No	ns	-320.0	550.5
2 vs 5	-79.04	0.86	No	ns	-367.7	209.7
2 vs 6	-71.19	0.75	No	ns	-368.5	226.1
3 vs 4	96.21	0.61	No	ns	-396.2	588.6
3 vs 5	-98.09	0.83	No	ns	-467.4	271.2
3 vs 6	-90.24	0.75	No	ns	-466.3	285.8
4 vs 5	-194.30	1.37	No	ns	-638.1	249.5
4 vs 6	-186.50	1.30	No	ns	-635.9	263.0
5 vs 6	7.84	0.08	No	ns	-301.9	317.6
KIF1B						
0 vs 1	-15.06	0.09	No	ns	-552.7	522.6
0 vs 2	-8.04	0.06	No	ns	-433.1	417.0
0 vs 3	-74.14	0.50	No	ns	-539.8	391.5
0 vs 4	-46.46	0.29	No	ns	-544.2	451.3
0 vs 5	-265.40	1.96	No	ns	-690.4	159.7
0 vs 6	-211.90	1.52	No	ns	-650.9	227.1
1 vs 2	7.02	0.05	No	ns	-418.0	432.1
1 vs 3	-59.08	0.40	No	ns	-524.7	406.6
1 vs 4	-31.40	0.20	No	ns	-529.2	466.4
1 vs 5	-250.30	1.85	No	ns	-675.4	174.7
1 vs 6	-196.80	1.41	No	ns	-635.8	242.2
2 vs 3	-66.10	0.63	No	ns	-395.3	263.2
2 vs 4	-38.42	0.32	No	ns	-411.8	334.9
2 vs 5	-257.30	3.01	No	ns	-526.2	11.5
2 vs 6	-203.80	2.21	No	ns	-494.2	86.5
3 vs 4	27.67	0.21	No	ns	-391.3	446.6
3 vs 5	-191.20	1.83	No	ns	-520.5	138.0
3 vs 6	-137.70	1.25	No	ns	-484.8	209.3
4 vs 5	-218.90	1.84	No	ns	-592.2	154.4
4 vs 6	-165.40	1.34	No	ns	-554.5	223.7
5 vs 6	53.50	0.58	No	ns	-236.9	343.9
KIF21B						
0 vs 1	14.89	0.17	No	ns	-264.8	294.5
0 vs 2	-18.04	0.26	No	ns	-236.2	200.1
0 vs 3	-87.39	1.13	No	ns	-329.6	154.8
0 vs 4	-1.50	0.02	No	ns	-260.4	257.4
0 vs 5	-93.94	1.33	No	ns	-316.2	128.3
0 vs 6	-140.0	1.95	No	ns	-364.9	85.0
1 vs 2	-32.93	0.47	No	ns	-251.1	185.2

1 vs 3	-102.30	1.33	No	ns	-344.5	139.9
1 vs 4	-16.39	0.20	No	ns	-275.3	242.5
1 vs 5	-108.80	1.54	No	ns	-331.1	113.4
1 vs 6	-154.9	2.16	No	ns	-379.8	70.1
2 vs 3	-69.35	1.30	No	ns	-236.8	98.1
2 vs 4	16.54	0.27	No	ns	-174.3	207.4
2 vs 5	-75.90	1.74	No	ns	-213.0	61.2
2 vs 6	-121.90	2.71	No	ns	-263.4	19.5
3 vs 4	85.89	1.24	No	ns	-132.0	303.8
3 vs 5	-6.55	0.12	No	ns	-179.3	166.2
3 vs 6	-52.58	0.94	No	ns	-228.8	123.6
4 vs 5	-92.44	1.48	No	ns	-287.9	103.1
4 vs 6	-138.50	2.19	No	ns	-337.0	60.1
5 vs 6	-46.04	0.98	No	ns	-193.7	101.6

Supplementary Table 2. Multiple regression analysis of KIF1B, age and Aβ protein expression

KIF protein	Sample type	n	Variables	Coefficient	Standard error	t	p value	95% Confidence intervals	
KIF1B	**Control**	32	***Age at death***	-0.60	0.49	-1.23	0.23	-1.59	0.40
			AβPP	-1.54	1.66	-0.93	0.36	-4.93	1.84
	AD	40	***Age at death***	-3.04	1.16	-2.61	0.01	-5.40	-0.68
			AβPP	-4.10	1.37	-3.00	0.01	-6.87	-1.33
KIF1B	**Control**	22	***Age at death***	-0.32	0.82	-0.39	0.70	-2.04	1.41
			Insoluble Aβ	91.04	65.26	1.40	0.18	-45.54	227.63
	AD	38	***Age at death***	-0.05	0.02	-2.89	0.01	-0.08	-0.01
			Insoluble Aβ	0.00	0.00	1.09	0.28	-0.00	0.00
KIF1B	**Control**	19	***Age at death***	-0.21	0.89	-0.24	0.81	-2.11	1.68
			Soluble Aβ	-0.35	13.84	-0.03	0.98	-29.69	28.99
	AD	37	***Age at death***	-0.04	0.16	-2.53	0.02	-0.07	-0.01
			Soluble Aβ	-0.31	0.16	-1.90	0.07	-0.64	0.02

Significant correlations highlighted in red. Aβ: amyloid-β; AD: Alzheimer's disease, AβPP: amyloid β protein precursor; KIF: kinesin superfamily motor protein.

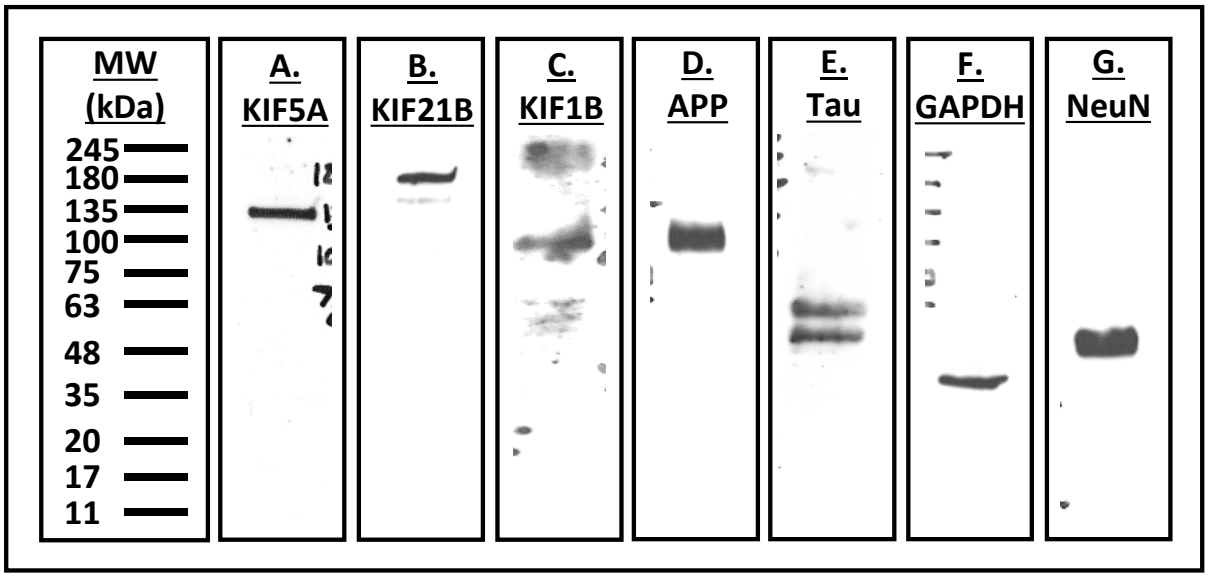

Supplementary Figure 1. Antibody specificity. Western blots were performed using Alzheimer's disease protein homogenates, derived from frontal lobe, to determine antibody specificity. Predicted molecular weight of KIF5A 107kDa and 117kDa. Antibody used for band detection was rabbit anti-KIF5A 1:1000; Sigma-Aldrich; HPA004469 (A). Predicted molecular weight of KIF21B 180kDa. Antibody used for detection was rabbit anti-KIF21B 1:1000; Sigma-Aldrich; HPA027274 (B). Predicted molecular weight of KIF1B 200kDa. Antibody used for detection was rabbit anti-KIF1B 1:1500; Bethyl Laboratories; A301-055A (C). Predicted molecular weight of APP 110kDa. Antibody used for detection was mouse anti-APP 1:2000; Zymed; 13-0200 (D). Predicted molecular weight of Tau 45-65kDa. Antibody used for detection was mouse anti-PHF-Tau 1:500; Thermoscientific; MN1020 (E). Predicted molecular weight of GAPDH 37kDa. Antibody used for detection was mouse anti-GAPDH 1:10,000; Abcam; Ab9484 (F). Predicted molecular weight of NeuN 48kDa. Antibody used for detection was rabbit anti-NeuN 1:5000; Abcam; Ab177487 (G). APP: amyloid precursor protein; GAPDH: Glyceraldehyde 3-phosphate dehydrogenase; kDa: kilodaltons; KIFs: kinesin superfamily proteins; MW; molecular weight; NeuN: neuronal nuclei.